Title

dCas9-based epigenome editing suggests acquisition of histone methylation is not sufficient for target gene repression.

Journal

Nucleic acids research, 45(17)

ISSN

0305-1048

Authors

O'Geen, Henriette
Ren, Chonghua
Nicolet, Charles M
et al.

Publication Date

2017-09-01

DOI

10.1093/nar/gkx578

Peer reviewed

Published online 4 July 2017

Nucleic Acids Research, 2017, Vol. 45, No. 17 ***9901–9916***
doi: 10.1093/nar/gkx578

dCas9-based epigenome editing suggests acquisition of histone methylation is not sufficient for target gene repression

Henriette O'Geen[1,†], Chonghua Ren[1,2,†], Charles M. Nicolet[3], Andrew A. Perez[3], Julian Halmai[1], Victoria M. Le[1], Joel P. Mackay[4], Peggy J. Farnham[3] and David J. Segal[1,*]

[1]Genome Center and Department of Biochemistry and Molecular Medicine, University of California, Davis, CA 95616, USA, [2]Guangzhou Key Laboratory of Insect Development Regulation and Application Research, School of Life Sciences, South China Normal University, Guangzhou 510631, China, [3]Department of Biochemistry and Molecular Medicine, Keck School of Medicine, University of Southern California, Los Angeles, CA 90089, USA and [4]School of Life and Environmental Sciences, The University of Sydney, Sydney, NSW 2006, Australia

Received February 11, 2017; Revised June 12, 2017; Editorial Decision June 15, 2017; Accepted June 28, 2017

ABSTRACT

Distinct epigenomic profiles of histone marks have been associated with gene expression, but questions regarding the causal relationship remain. Here we investigated the activity of a broad collection of genomically targeted epigenetic regulators that could write epigenetic marks associated with a repressed chromatin state (G9A, SUV39H1, Krüppel-associated box (KRAB), DNMT3A as well as the first targetable versions of Ezh2 and Friend of GATA-1 (FOG1)). dCas9 fusions produced target gene repression over a range of 0- to 10-fold that varied by locus and cell type. dCpf1 fusions were unable to repress gene expression. The most persistent gene repression required the action of several effector domains; however, KRAB-dCas9 did not contribute to persistence in contrast to previous reports. A 'direct tethering' strategy attaching the Ezh2 methyltransferase enzyme to dCas9, as well as a 'recruitment' strategy attaching the N-terminal 45 residues of FOG1 to dCas9 to recruit the endogenous nucleosome remodeling and deacetylase complex, were both successful in targeted deposition of H3K27me3. Surprisingly, however, repression was not correlated with deposition of either H3K9me3 or H3K27me3. Our results suggest that so-called repressive histone modifications are not sufficient for gene repression. The easily programmable dCas9 toolkit allowed precise control of epigenetic information and dissection of the relationship between the epigenome and gene regulation.

INTRODUCTION

While genomic DNA holds the key to the genetic code, epigenetics offers another layer of information that establishes cell fate during development, aging and disease as well as in response to the environment. Epigenetics is a means by which the transcriptome (and thus the proteome) of a cell can be changed without alteration of the genetic content. Epigenetic regulation is thought to be accomplished through epigenetic marks such as post-translational modifications of histones and DNA methylation, and also via other mechanisms involving non-coding RNAs (1,2). Regions of active gene expression and open chromatin carry a signature of epigenetic marks that is distinct from repressed and heterochromatic regions (2). For example, histone acetylation is always associated with active transcription, while different histone methylation marks are associated with active versus repressed chromatin. Specifically, tri-methylation of lysine 4 on histone H3 (H3K4me3) is associated with active transcription, while tri-methylation of H3K9 (H3K9me3) and H3K27 (H3K27me3) are associated with repressed chromatin regions. There has been a significant effort to decipher the relationship between epigenetic marks, regulatory element activity and gene regulation. Large consortia projects such as ENCODE and the Roadmap Epigenomics Project have mapped epigenetic signatures across the human genome in many different cell types and tissues, which have then been correlated with gene expression (3,4). These association-based studies have provided epigenomic landscapes of epigenetic marks present at promoters and other regulatory elements, but cannot dissect the dynamic relationships between the epigenome and transcriptional control. While some evidence suggests that silencing of gene expression precedes *de novo* DNA methy-

*To whom correspondence should be addressed. Tel: +1 530 754 9134; Fax: +1 530 754 9658; Email: djsegal@ucdavis.edu
†These authors contributed equally to the paper as first authors.

lation (5), the causal relationship between the presence of a histone mark and gene expression is still unclear.

Epigenome editing is an emerging tool to alter epigenetic marks at defined genomic loci (6). Precise DNA targeting was first accomplished with the design of programmable proteins based on zinc fingers (ZFs) and Transcription Activator-Like Effectors (TALEs) (7,8). However, the field has been revolutionized by the discovery of the RNA-guided DNA-targeting platform CRISPR/Cas9 (clustered, regularly interspaced, short palindromic repeat/CRISPR-associated protein 9) (9,10). The platform consists of the Cas9 nuclease protein and a single guide RNA (sgRNA) that allows the nuclease to bind a specific DNA sequence through RNA–DNA base pairing. The most commonly used Cas9, from *Streptococcus pyogenes*, is only limited by the requirement of a 5′-NGG-3′ protospacer-adjacent motif (PAM) immediately adjacent to a 20-nt DNA target sequence (11,12). Two single amino acid mutations in Cas9 (D10A, H840A) abolish its nuclease activity, giving rise to an RNA-guided DNA-binding protein that lacks enzymatic activity (dCas9) (10). dCas9 can be fused to heterologous effector domains to regulate transcription in a highly specific manner (13–15).

There has been considerable recent focus on dCas9-tethered epigenetic enzymes that alter DNA methylation. In particular, dCas9 fusions to DNMT3A/B or TET1/2 have been shown to target the deposition of 5-methylcytosine (5-mC) or the acquisition of 5-hydroxy-mC (5-hmC, considered to be the initial step in the removal of DNA methylation), respectively (16–21). Fewer studies have explored dCas9 fusions with enzymes affecting histone modifications. Gene activation has been explored using the histone acetyltransferase p300, histone demethylase LSD1 and a H3K4 methylase (22–24). Gene repression has been attempted using dCas9-KRAB fusions (15,25). The Krüppel-associated box (KRAB) domain recruits endogenous chromatin modifying complexes including the KAP1 co-repressor complex (26,27) and the nucleosome remodeling and deacetylase (NuRD) complex (28) and thus has the potential to both tri-methylate histone H3 on lysine 9 and to deacetylate histones. Catalytic domains from several other enzymes that catalyze H3K9me3 (such as G9A and SUV39H1) have been linked to either ZF or TALE DNA-binding domains, causing repression of the *HER2* gene promoter (29). Although H3K27me3 is associated with repression, Ezh2 (the catalytic subunit of the Polycomb repressive complex 2 (PRC2) that causes deposition of H3K27me3) has not yet been studied as a fusion to a programmable DNA-binding domain. Importantly, in these previous studies, only changes in gene expression were used to assess the efficacy of the targeted epigenetic regulators. Few studies have monitored the changes in histone modification at the target site bound by the epigenetic regulator. However, such studies are essential to dissect the cause-and-effect relationship between histone modifications and transcriptional regulation.

In this study, we investigated a broad set of epigenetic enzymes (epigenetic writers) and epigenetic recruiters (peptides or proteins recruiting chromatin modifying complexes) designed for producing transcriptionally repressive histone marks when fused to a common dCas9 platform. In addition to well-studied writers of H3K9me3 (G9A, SUV39H1) and the KRAB repressor domain (6,30), we also created and used fusions to Ezh2 (a writer of H3K27me3) and to the N-terminal 45 residues of Friend of GATA-1 (FOG1), which has been associated with acquisition of H3K27me3 and loss of histone acetylation, (31,32); these domains have not been previously investigated as dCas9 fusions. The effects of the marks introduced by these proteins on gene expression were compared to the effects of DNA methylation by dCas9-DNMT3A. We show that dCas9 fusions to catalytic domains of EZH2, G9A and SUV39H1, as well as dCas9 fused to the N terminus of FOG1, are sufficient for some level of repression of three different promoters in two different cell types, but that repression is not always correlated with the expected histone modification. We show that the dCas9-like targeting protein dCpf1 was not able to substitute for dCas9 in these experiments. Finally, we show that combinations of targeted effectors can produce persistent silencing.

MATERIALS AND METHODS

Construction of dCas9 expression plasmids

A variety of epigenetic effectors were fused to human codon-optimized and catalytically inactive 'dead' Cas9 (dCas9) in different conformations. The improved pCDNA3-dCas9 expression plasmid was obtained by altering the original dCas9 plasmid (33) using Gibson cloning. The improved pCDNA3-dCas9 contains two nuclear localization signals, a 3× Flag epitope tag as well as [$(GGS)_5$] amino acid linkers at the N- and C-terminus of dCas9 with flanking restriction sites KpnI and NheI, respectively. Improved dCas9 protein sequence is shown in Supplementary Figure S1. Effector domains were amplified using 2× Phusion Master Mix (New England Biolabs) according to the manufacturer's instructions. Polymerase chain reaction (PCR) primers for cDNA amplification of individual effector domains were designed with cloning vector overhangs for Gibson cloning. All primers are listed in Supplementary Table S1. cDNA for G9A[SET], SUV[SET] and DNMT3A was kindly provided by the lab of Marianne Rots (29,34). DNMT3L expression plasmid pCDNA-DNMT3L was a kind gift from Dr Fred Chedin (35). Mouse Ezh2[FL] cDNA was synthesized by Bio Basic Inc. Ezh2[FL] was used as a template to amplify the shorter Ezh2[SET] domain. Catalytic mutants Ezh2[SET-Y641A]-dCas9 and Ezh2[SET-Y726F]-dCas9 were created by site-directed mutagenesis using the QuikChange II XL Site-Directed Mutagenesis kit (Stratagene). Primers used for mutagenesis are listed in Supplementary Table S1. KRAB domain was amplified from dCas9-KRAB (33) and FOG1 cDNA was amplified from HEK293FT cells. Total RNA was isolated from HEK293FT using the RNeasy mini kit (Qiagen) and cDNA was synthesized using random hexamer primers using the RevertAid cDNA synthesis kit (ThermoScientific). Using Gibson Assembly (New England Biolabs), amplified cDNAs were cloned into either KpnI or NheI digested dCas9 vector for N-terminal or C-terminal fusions to dCas9, respectively. Finally, the FOG1 epigenetic effector construct was Gibson assembled (New England Biolabs). Protein sequences of dCas9-fusions are supplied

in Supplementary Figure S1. For array of two, three and four FOG1 domains to the N-terminus of dCas9, FOG1 monomer coding sequences were amplified separately by PCR introducing a GS linker between individual monomer coding sequences and the KpnI and FseI restriction sites at the beginning of first monomer and the end of the last monomer for each array. In addition, a BsaI endonuclease site was added to either end of the FOG1 monomers and each fragment contains a distinct four-base overhang that directs the assembly of multiple monomers. Amplification primers are listed in Supplementary Table S1. Two, three or four monomer coding sequences were mixed with pFusA plasmid for Golden Gate Assembly cloning with BsaI and T4 DNA ligase (New England Biolabs). DNA fragments of arrays of two, three and four FOG1 domains were digested with KpnI and FseI and ligated into the KpnI/FseI digested dCas9 plasmid.

Cloning of expressing plasmid

The cloning vector was obtained from Addgene (36, Addgene plasmid # 41824) and was linearized using the AflII restriction enzyme. A total of 19-bp gRNA target sequences were selected within 500 bp of the relevant gene promoter using the online tool CHOPCHOP (37). Each gRNA sequence was selected and incorporated into two 60mer oligonucleotides that contained cloning vector overhangs for Gibson assembly. After annealing and extending the oligonucleotides to 100-bp, the PCR purified (PCR purification kit; QIAGEN) dsDNA was Gibson assembled into the AflII linearized plasmid. Oligomers used to create target-specific vectors are listed in Supplementary Table S2.

Construction of dCpf1 expression plasmids and crRNA

The inactive Cpf1 was generated by mutating the catalytic domain *As*Cpf1 (D908A; (38)). This amino acid change was induced through adding mutations in the primers during PCR amplification with pcDNA3.1-hAsCpf1 (Addgene, plasmid #69982) as template. Primers are listed in Supplementary Table S3. Two PCR fragments were inserted into the FseI/NheI linearized pCDNA3-dCas9 backbone using Gibson assembly thereby replacing dCas9 with dCpf1. Effector domains were then added using KpnI and/or NheI digested plasmid to generate N- and/or C-terminal dCpf1 fusions following the same principle as dCas9 fusions. This step uses the same cDNA amplification primers as described for dCas9 fusions. crRNA was designed to target 23-bp adjacent to the 5′-NTTT-3′ PAM. crRNA target sequence is listed in Supplementary Table S3. For Cpf1 cleavage assays and dCpf1 chromatin immunoprecipitation (ChIP) assays, we amplified the U6-crRNA cassette by PCR (39). The U6-crRNA cassette was then co-transfected with dCpf1 expressing plasmids as described below. To determine repression by dCpf1 fusion proteins we co-expressed plasmids containing the U6-crRNA cassette with plasmids expressing dCpf1 fusions (40).

Cell lines and transfection

The human colon cancer cell line HCT116 (ATCC #CCL-247) was grown in McCoy's 5A Medium supplemented with 10% fetal bovine serum and 1% penicillin/streptomycin. Cells were maintained at 37°C and 5% CO_2. HCT116 cells were authenticated by the Bioreagent and Cell Culture Core, USC Norris Comprehensive Cancer Center. Cells of 50–60% confluency were transfected using Lipofectamine 3000 (Life Technologies) following the manufacturer's instructions. Transfections for RNA extraction were performed in 12-well plates using 625 ng dCas9 expression vector, 500 ng of equimolar pooled expression vectors and 125 ng pBABE-puro. Transfections with dCpf1 were carried out using the same protocol except that U6-crRNA expressing plasmids were co-transfected with dCpf1 expressing plasmids as described elsewhere (39). For ChIP assays and DNA-methylation analysis, cells were plated in 10-cm^2 culture dishes and transfection scaled up accordingly. Transfection medium was replaced 24 h post-transfection with growth medium containing 3 μg/ml puromycin to enrich for transfected cells. Subsequently, puromycin-containing media was exchanged every 24 h. To assay for persistent repression, media was switched to standard growth media four days after transfection.

RNA extraction and reverse-transcription quantitative PCR (RT-qPCR)

Transfected cells were rinsed in 1×DPBS and RNA stabilized by adding 500 μg RNAlater (Ambion) and stored at 4°C for up to 1 week. Total RNA was extracted 3–4 days after transfection using the RNeasy Mini kit (QIAGEN) and 500 ng RNA were reverse-transcribed using the SuperScript VILO MasterMix (Invitrogen) according to the manufacturer's instructions. Real-time PCR was performed in triplicate with 2× iQ SYBR mix (Bio-Rad) using the CFX384 Real-Time System C1000 Touch Thermo Cycler (BioRad) and the included software was used to extract raw Cq values. Gene expression analysis was performed with *GAPDH* as a reference gene in at least two biological replicates using intron-spanning *HER2* primers (HER2-F 5′-GGGAAACCTGGAACTC ACCT-3′; HER2-R 5′-GACCTGCCTCACTTGGTTGT-3′), *EPCAM* primers (EPCAM-F 5′-CTGGCCGTAAAC TGCTTTGT-3′; EPCAM-R 5′- TCCCAAGTTTTGAG CCATTC-3′), *MYC* primers (MYC-F 5′- AAACACAAAC TTGAACAGCTAC-3′; MYC-R 5′-ATTTGAGGCAGT TTACATTATGG-3′) and *GAPDH* primers (GAPDH-F 5′-AATCCCATCACCATCTTCCA-3′; GAPDH -R 5′-CT CCATGGTGGTGAAGACG-3′). Relative target gene expression was calculated as the difference between the target gene and the *GAPDH* reference gene (dCq = Cq[target]-Cq[*GAPDH*]). Gene expression results are indicated as fold change to a reference sample (usually dCas9 without any effector domain), using the ddCq method. We applied a one-way ANOVA (ANalysis Of VAriance) with post-hoc Tukey HSD (Honestly Significant Difference) test to determine statistical significance for different dCas9 fusions.

Chromatin immunoprecipitation (ChIP)-qPCR

For ChIP assays of histone marks, transfected cells were cross-linked 3–4 days post transfection by incubation with 1% formaldehyde solution for 10 min at room temperature

and the reaction was stopped by the addition of glycine to a final concentration of 125 mM. Cross-linked cell pellets were stored at −80°C. Chromatin was extracted and ChIP performed using StaphA cells (Sigma–Aldrich, St Louis, MO, USA) to collect the immunoprecipitates as previously described (33,41) Briefly, chromatin was sheared to an average fragment size of 500-bp using a Bioruptor 2000 (Diagenode). A total of 10 μg chromatin were used per ChIP assay. ChIP enrichment was performed by incubation with 3 μg H3K9me3 antibody (Abcam ab8898), 3 μg H3K9me2 antibody (MP 07–441), 2 μg H3K27me3 antibody (MP 07–449), 2 μg H3K27ac antibody (Active Motif #39133) or 2 μg normal rabbit IgG (Abcam ab46540) for 16 h at 4°C. Immuno complexes were bound to StaphA cells for 15 min at room temperature. For dCpf1 and dCas9 ChIP assays, HCT116 cells were transfected in 10 cm culture dishes as described above, but puromycin selection was omitted. After cross-linking of chromatin, ChIP assays were performed using 3 μg Flag antibody (SIGMA M2 F1804) at 4°C overnight. Immuno complexes were captured with 3 μg rabbit anti mouse antibody for 1 h at 4°C and were bound to StaphA cells for 15 min at room temperature. After washing and reversal of cross-links DNA was purified using the QIAquick PCR Purification Kit (Qiagen). ChIP-DNA and diluted Input control were used for subsequent qPCR reactions with 2× SYBR FAST mastermix (KAPA Biosystems) according to the manufacturer's recommendations using the CFX384 Real-Time System C1000 Touch Thermo Cycler (BioRad). ChIP enrichment was calculated relative to input samples using the dCq method (dCq = Cq[*HER2*-ChIP]-Cq[input]). *HER2* ChIP amplification primers are as follows: HER2-ChIP-F (5′-TTGGAATGCAGTTGGAGGGG-3′) and HER2-ChIP-R (5′-GGTTTCTCCGGTCCCAATGG-3′). We applied a one-way ANOVA (ANalysis Of VAriance) with post-hoc Tukey HSD (Honestly Significant Difference) test to determine statistical significance for different dCas9 fusions.

DNA-methylation analysis

Genomic DNA from transfected and untreated cells was isolated using the Quick-gDNA MiniPrep kit (ZYMO). Bisulfite conversion was performed using the EZ DNA Methylation-Lightning Kit (ZYMO) following the manufacturer's instructions. Bisulfite-Sequencing PCR primers (HER2-BSP-F 5′-GGAGGGGGTAGAGTTATTAGTTTTT-3′ and HER2-BSP-R 5′-AAATAACAACTCCCAACTTCACTTT-3′) were designed using MethPrimer (42). Bisulfite converted DNA was used for PCR amplification with GoTaq polymerase (Promega) and the 152-bp PCR product was purified with the QIAquick PCR Purification Kit (Qiagen). Amplicons were inserted into the pCR4-TOPO TA vector using the TOPO-TA-cloning kit (ThermoFisher) and transformed into NEB5α competent cells. Plasmid DNA from individual recombinant clones was isolated and subjected to Sanger sequencing using M13F primers at the College of Biological Sciences UC DNA Sequencing Facility. Methylation status of CpGs for each clone was determined by sequence comparison.

Single-strand annealing (SSA) recombination reporter assay

For the pPGK-mCherry reporter plasmid, the Cpf1 nuclease binding site (crRNA binding region on *HER2* promoter) was inserted between *Xho*I/*Bam*HI sites, which is flanked with 200-bp direct repeats derived from mCherry as single-strand annealing (SSA) arms (43). The open reading frame of the mCherry gene was interrupted by the insertion of the relevant binding region and a series of three stop codons (Supplementary Figure S2A). Nucleases causing double strand breaks at the target site induce SSA repair, which leads to expression of functional mCherry protein that can readily be detected by its fluorescence (Supplementary Figure S2B). To evaluate cleavage activity, pcDNA3-Cpf1 and pcDNA3-dCpf1, were co-transfected with the three PCR amplified U6-crRNAs cassette and the mCherry reporter plasmid in HEK293T cells. Cells were observed 48 h post-transfection.

Western blot analysis

Transfected cells were lysed 48 h post-transfection in 1×RIPA buffer (Millipore) supplemented with protease inhibitor cocktail (Roche). Protein concentrations were determined by Bradford assay (BioRad) and 20 μg protein were separated on a 4–15% TGX^{TM} gel (BioRad) in Tris/Glycine/Sodium dodecyl sulphate buffer and transferred onto nitrocellulose membranes. Protein loading was evaluated by Ponceau S stain. After rinsing the membrane with deionized water, non-specific antigen binding was blocked in TBST buffer (50 mM Tris, 150 mM NaCl and 0.1% Tween-20) with 5% nonfat dry milk (Cell Signaling). Membranes were incubated with primary antibody in blocking solution at 4°C over night. We used monoclonal antibodies against Flag (1:1000; SIGMA M2 F1804) or anti beta-actin (1:2500; SIGMA A5441). Membranes were washed with TBST three-times for 10 min before membranes were incubated with horseradish peroxidase conjugated anti mouse secondary antibody at room temperature. After 45 min, the membrane was washed three-times in TBST and proteins were visualized with Amersham ECL Prime Western Blotting Detection Reagent (GE Healthcare) and autoradiobiography film.

RESULTS

Systematic evaluation of repression by dCas9 fused to catalytic domains of histone lysine methyltransferases G9A and SUV39H1

Epigenetic effector domains for H3K9 methylation have been previously fused to artificial ZF proteins (ZFP) to affect transcriptional regulation in a targeted manner. More specifically, the C-terminal end of ZFP E2C, which targets the *HER2* promoter, had been previously fused to the catalytic SET (Su(var)3-9, Enhancer-of-zeste and Trithorax) domains of the histone methyltransferases (HMT) G9A or SUV39H1 (here referred to as G9A[SET] and SUV[SET], respectively; Figure 1A), and was shown to repress endogenous *HER2* gene expression (29). In order to test the framework for the repressive and epigenetic activity of RNA-guided dCas9 fusions, we fused G9A[SET] and SUV[SET]

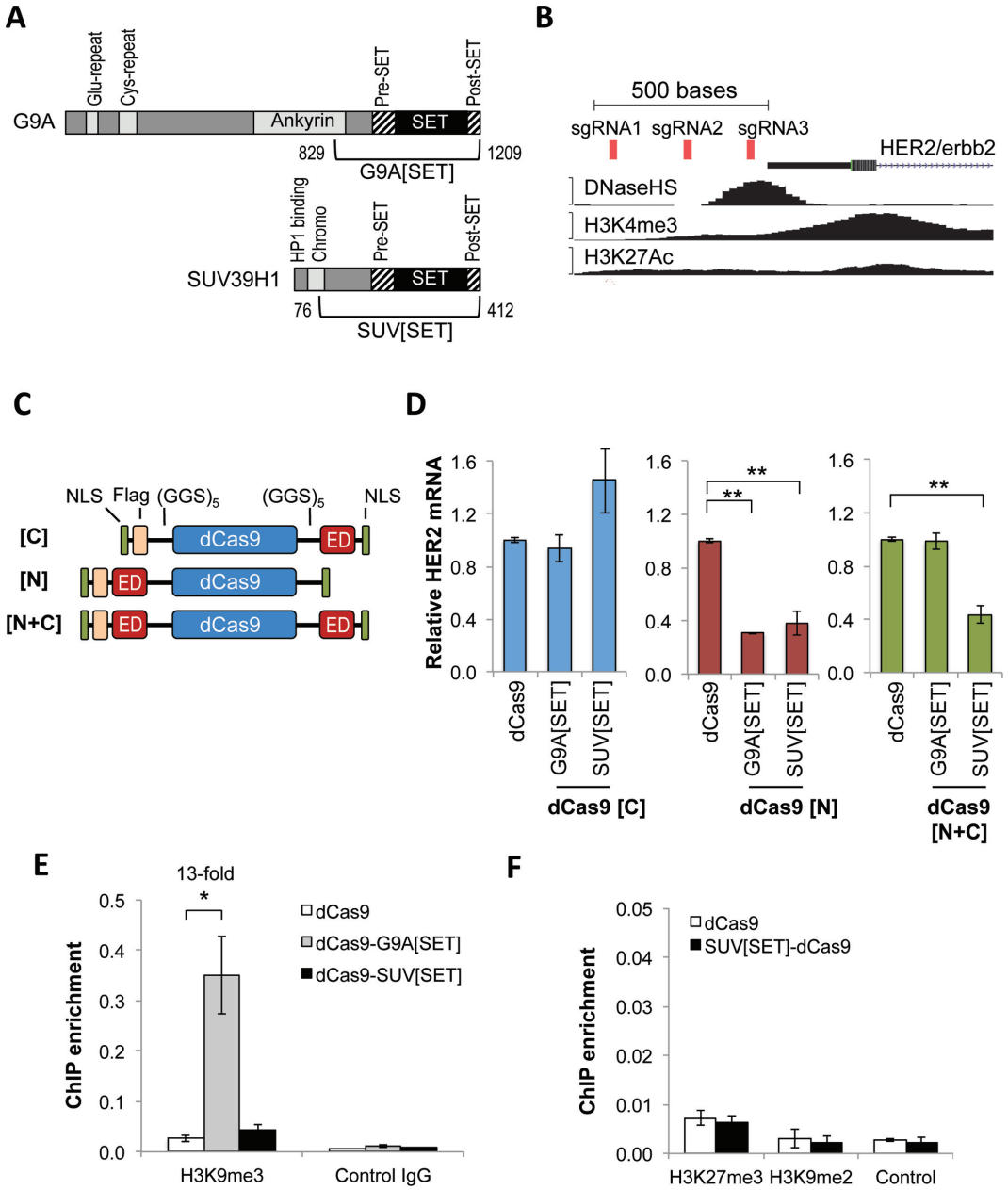

Figure 1. N-terminal fusions of H3K9 methyltransferases to dCas9 repress *HER2* gene expression independent of histone methylation. (**A**) Schematic representation of the H3K9 histone methyltransferases (HMT) G9A and SUV39H1, with protein domains indicated. Regions that were fused to dCas9 are labeled as G9A[SET] and SUV[SET]. (**B**) The genomic target sites of the three that target dCas9 to a 500-bp region of the *HER2* promoter. ENCODE tracks of DNaseHS, H3K4me3 and H3K27A in HCT116 are shown. (**C**) The design of dCas9 fusion proteins. dCas9 fusions contained N-terminal and C-terminal nuclear localization domains (NLSs), as well as an N-terminal 3XFLAG epitope tag. dCas9 fusion proteins contained the histone methyltransferase effector domain (ED) at the N-terminus, C-terminus or both the N- and C-termini (labeled [N], [C] and [N+C], respectively). A 15-aa linker [$(GGS)_5$] separates the dCas9 and the EDs. (**D**) Relative *HER2* mRNA levels resulting from dCas9-ED fusions compared to dCas9 with no ED was determined by RT-qPCR in HCT116 cells after co-transfection of plasmids expressing the indicated dCas9 fusions with the three sgRNAs targeted to the *HER2* promoter (Tukey-test, $P < 0.01$, $n = 2$ independent experiments each; mean ± SEM). (**E**) H3K9me3 ChIP-qPCR enrichment at the *HER2* promoter in HCT116 cells co-transfected with three sgRNAs targeted to the *HER2* promoter and the indicated N-terminal dCas9 fusions (Tukey test, $*P < 0.05$, $n = 2$ independent experiments; mean ± SD). The number above the bar indicates the fold-increase in H3K9me3 enrichment relative to dCas9 with no ED. ChIP assays using normal rabbit IgG were used as negative controls. (**F**) ChIP-qPCR enrichment of K3K27me3 and H3K9me2 at the *HER2* promoter in HCT116 cells co-transfected with three sgRNAs and the indicated dCas9 fusions (No comparisons were significant, $n = 2$ independent experiments; mean ± SD).

to dCas9 and used three single-guide (sg)RNAs simultaneously to target the dCas9 fusions to the promoter of *HER2* (Figure 1B and Supplementary Table S2). Effector domains were fused to either the N-terminus, the C-terminus or both the N- and C-termini of dCas9 to determine the most effective configuration for the dCas9-fusions (Figure 1C). Crystal structures have revealed that neither the N-terminus nor C-terminus of dCas9 is in immediate proximity to its bound DNA (44). We therefore introduced a linker of 15 amino acids [$(GGS)_5$] between dCas9 and the effector domain to improve the ability of the effector domain to contact the DNA or histones. Surprisingly, we found that the domains fused to the C-terminal end of dCas9 were unable to repress transcription, whereas both N-terminal fusions of G9A[SET]-dCas9 and SUV[SET]-dCas9 displayed 3.3- and 2.7-fold downregulation of *HER2* mRNA, respectively (Tuckey HSD test, $P < 0.01$; Figure 1D). Western blot analysis confirmed that N- and C-terminal dCas9-fusions were expressed at similar levels (Supplementary Figure S3A) and that differences in repressive activity were due to the configuration of the dCas9 fusions. Having effector domains at both the N- and C-terminus did not increase the repressive capacity. Specifically, the repressive capacity of SUV[SET]-dCas9-SUV[SET] (2.2-fold) was comparable to that of the single SUV[SET]-dCas9, while G9A[SET]-dCas9-G9A[SET] showed no repressive activity, suggesting that the C-terminal G9A[SET] attenuated the activity of the N-terminal fusion. Negative controls using a dCas9 with no effector domain but co-transfected with the three sgRNAs, or an mCherry reporter plasmid only, had no effect on *HER2* expression. Since N-terminal fusions of effector domains to dCas9 were most effective, we focused on these in subsequent experiments.

Repression by dCas9-SUV[SET] does not require tri-methylation of H3K9 at *HER2* gene promoter

To determine if repression by G9A[SET]-dCas9 and SUV[SET]-dCas9 is associated with tri-methylation of H3K9, we performed histone ChIP-qPCR assays to quantitatively measure H3K9me3 enrichment at the *HER2* promoter. ChIP enrichment was evaluated relative to dCas9 that did not contain an effector domain. G9A[SET]-dCas9 co-transfected with the three guide-RNAs produced a 13-fold increase in H3K9 tri-methylation compared to dCas9 with no ED (Tuckey HSD test, $P < 0.05$; Figure 1E), whereas SUV[SET]-dCas did not increase H3K9me3 levels. This result was surprising given that G9A[SET]-dCas9 and SUV[SET]-dCas9 caused similar levels of *HER2* repression (3.3- and 2.7-fold, respectively, Figure 1D). Therefore, although the SUV[SET] domain was sufficient to repress *HER2* transcription it was not sufficient to mediate H3K9me3 addition. Importantly, our data suggest that an increase in H3K9me3 at the target promoter was not required for SUV39H1-mediated repressive activity. Thus, some other activity of the SUV[SET] domain may have been responsible for the repression, since dCas9 alone did not cause repression. One possibility is that other repressive histone marks were deposited to cause the repression. This latter possibility was investigated by examining alternative histone marks that have been associated with repression. Neither H3K27me3 nor H3K9me2 marks changed at the *HER2* promoter when targeted by SUV[SET]-dCas9 (for which H3K9me3 was expected but not observed) (Figure 1F). The lack of deposition of expected or alternative repressive histone marks further supported the conclusion that repression by SUV[SET]-dCas9 did not require histone methylation.

Full-length histone methyltransferase Ezh2 is required for H3K27 methylation, but H3K27me3 is not correlated with repressive activity

H3K9me3 and H3K27me3 mark distinct regions in the genome (45); H3K9me3 is a mark typical of constitutive heterochromatin, while H3K27me3 is usually enriched on facultative heterochromatin (2,46). It is possible that an enzyme associated with the formation of facultative heterochromatin could be effective in modifying promoter activity. However, enzymes mediating the repressive H3K27me3 mark have not yet been targeted to a specific genomic locus by dCas9. We therefore created dCas9 N-terminal fusions with the full-length mouse methyltransferase (Ezh2[FL]), as well as a truncated form (Ezh2[SET]) containing the CXC and SET domains (aa482–746) but lacking some of the N-terminal domains (Figure 2A). Both Ezh2[FL]-dCas9 and Ezh2[SET]-dCas9 produced repression of *HER2* gene expression (1.6-fold [Tuckey HSD test, $P < 0.05$] and 2-fold [Tuckey HSD test, $P < 0.01$], respectively; Figure 2B). However, only Ezh2[FL]-dCas9 was able to deposit H3K27me3 at the *HER2* promoter, producing a 9-fold enrichment compared to dCas9 with no effector domain (Tukey HSD test, $P < 0.01$, Figure 2C). Therefore, similar to the case of SUV[SET]-dCas9, our data suggest that Ezh2 residues in addition to those in the CXC and SET domains may be required for H3K27 tri-methylation activity. We further tested if gene repression by Ezh2[SET]-dCas9 was associated with other known repressive histone marks. There was no increase in H3K9me2 or H3K9me3 that could explain the repression caused by Ezh2[SET]-dCas9 (for which H3K27me3 was expected but not observed) (Figure 2D). The lack of deposition of expected or alternative repressive histone marks again supported the conclusion that repression by Ezh2[SET]-dCas9 does not require histone methylation.

Taken together, our results support a hypothesis that neither H3K9me3 nor H3K27me3 must precede or are causative for repression. A possible non-epigenetic mechanism for repression was the simple steric interference of endogenous regulatory components by the binding of the dCas9-ED fusions. dCas9 alone did not cause repression by this mechanism, as cells transfected with only an mCherry expression plasmid displayed *HER* expression at a level similar to a dCas9 with no ED (Figure 3C). However, the repression displayed by the dCas9-ED fusions above suggests that these dCas9 appendages might produce interference. This non-catalytic mechanism was investigated using catalytic mutants of the Ezh2[SET] domain. Catalytic sites for the Ezh2 SET domain have been identified and defined by their ability to contact and methylate H3K27, including invariant residues involved in targeting lysine or S-adenosyl methionine (30,47). We there-

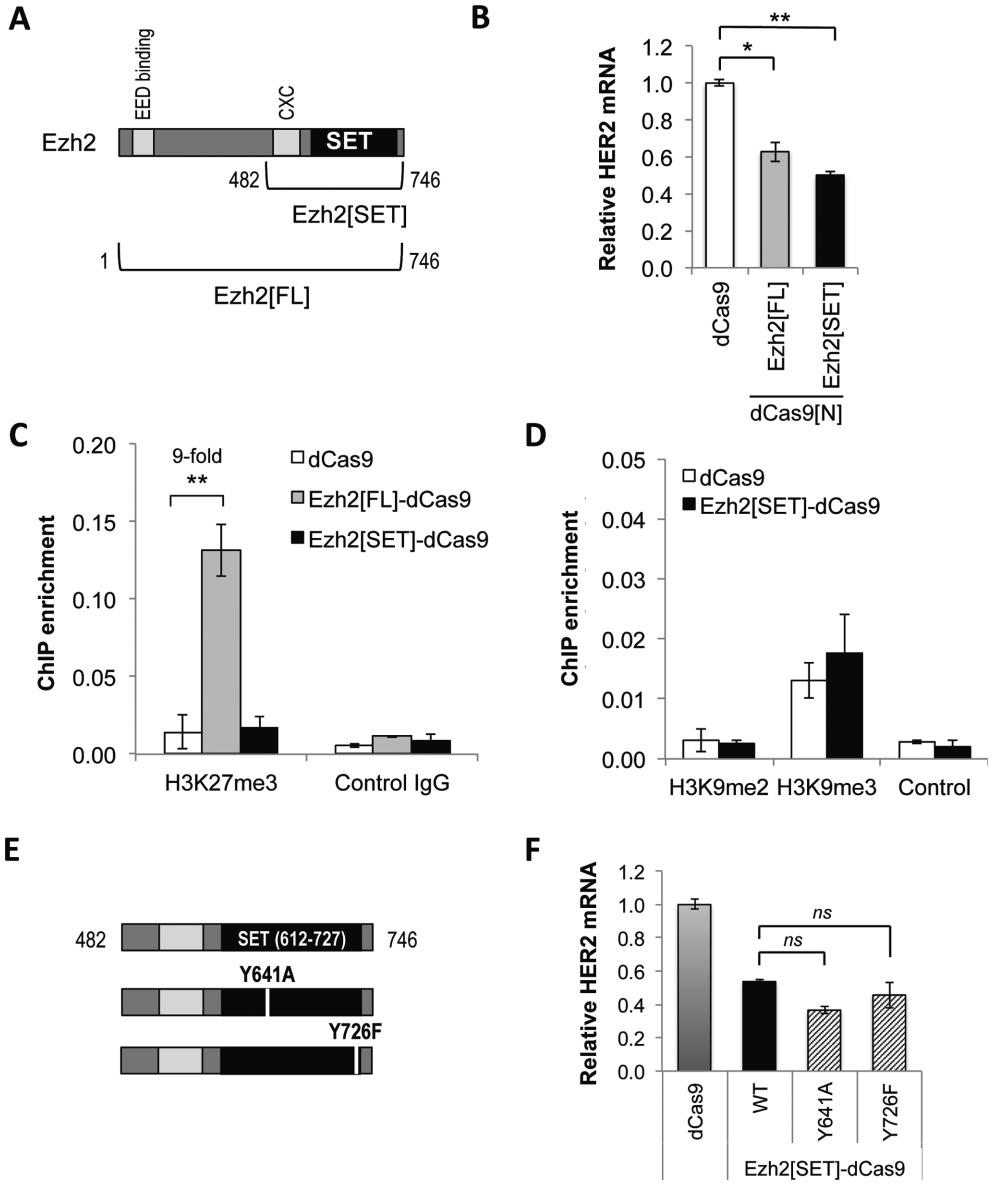

Figure 2. N-terminal fusions of Ezh2 H3K27 methyltransferases to dCas9 repress *HER2* gene expression independent of histone methylation. (**A**) Schematic representation of the H3K27 methyltransferase Ezh2. Regions of each protein fused to dCas9 are labeled Ezh2[SET] and Ezh2[FL], and protein domains are indicated. (**B**) Relative *HER2* mRNA production in cells co-transfected with a pool of three sgRNAs targeted to the *HER2* gene promoter and the indicated dCas9 fusions. Expression data are shown in comparison to cells transfected by dCas9 with no ED (Tukey-test, $*P < 0.05$, $**P < 0.01$, $n = 2$ independent experiments; mean ± SEM). (**C**) H3K27me3 enrichment was assessed for the indicated dCas9 fusion proteins as in Figure 1 (Tukey test, $P < 0.01$, $n = 2$ independent experiments; mean ± SD). (**D**) ChIP-qPCR enrichment of H3K9me2 and H3K9me3 at the *HER2* promoter in HCT116 cells, as in Figure 1F. (**E**) Schematic representation of Ezh2[SET] catalytic mutants. (**F**) Relative *HER2* mRNA production using the indicated Ezh2[SET]-dCas9 fusions. Expression data are shown in comparison to cells transfected by dCas9 with no ED (*ns*, not significant; $n = 2$ independent experiments; mean ± SEM).

fore mutated tyrosine 641 to alanine (Y641A) and tyrosine 726 to a phenylalanine (Y726F), creating Ezh2[SET-Y641A]-dCas9 and Ezh2[SET-Y726F]-dCas9, respectively (Figure 2E). If repressive activity is truly uncoupled from epigenetic writing activity, the mutant fusions should repress gene expression similarly to the catalytically active Ezh2[SET]. Indeed both, Ezh2[SET-Y641A]-dCas9 and Ezh2[SET-Y726F]-dCas9 repressed *HER2* expression similar to the wild-type Ezh2[SET]-dCas9 fusion (Figure 2F). These data strongly suggest that some or all of the repression observed using these dCas9-ED fusions could be due to non-catalytic mechanisms such as steric interference. However, since dCas9-G9A[SET] and Ezh2[FL]-dCas9 did clearly deposit their expected epigenetic mark, these latter data also reinforce that neither H3K9me3 nor H3K27me3 must precede or are causative for repression.

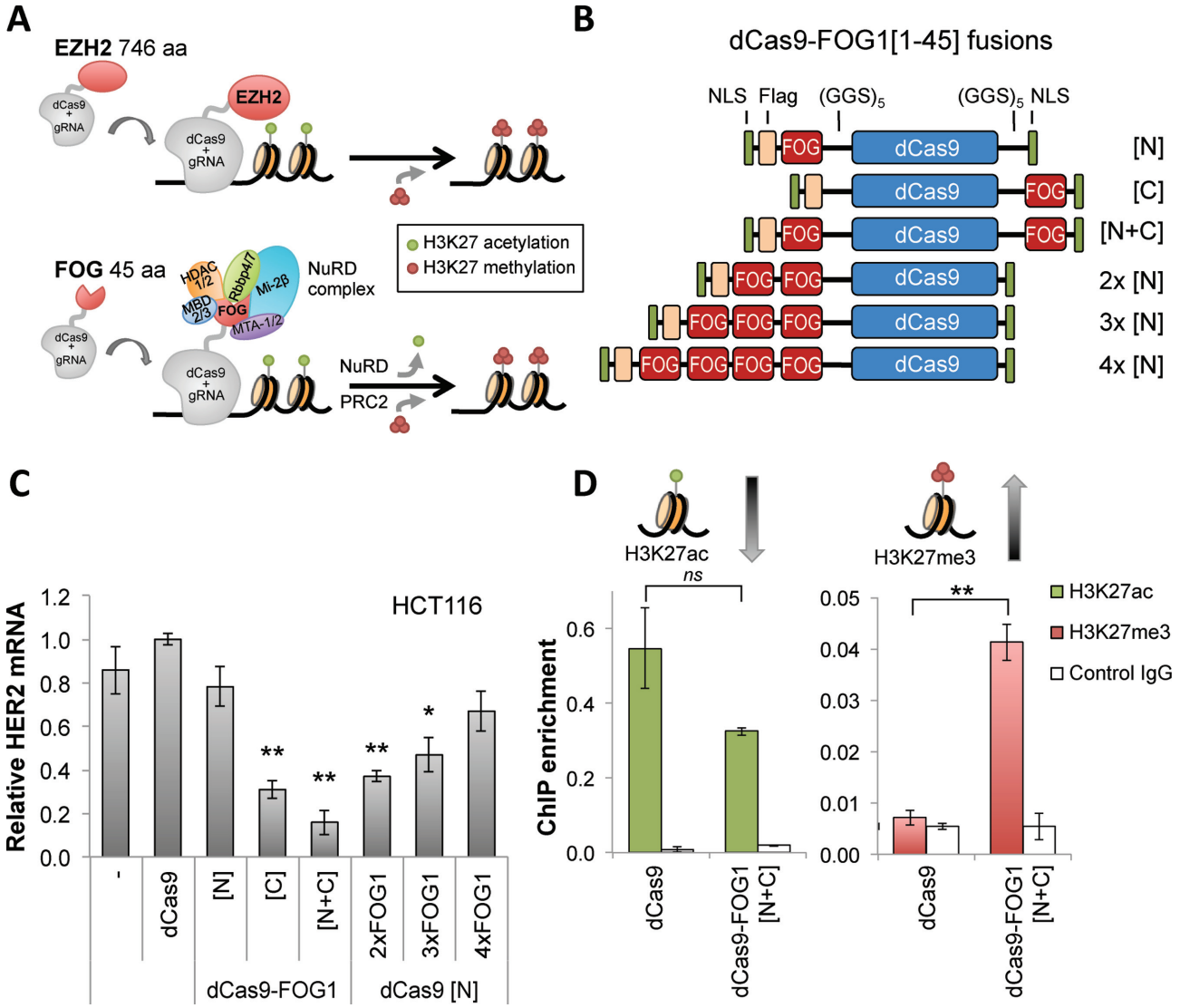

Figure 3. The novel transcriptional repressor FOG1[1–45]-dCas9-FOG1[1–45] tri-methylates H3K27 at the target promoter. (**A**) Models for two approaches of targeted H3K27 methylation mediated by dCas9-fusion proteins. Top**:** fusion of dCas9 to the enzyme Ezh2 directly tri-methylates H3K27 at the genomic target region. Bottom**:** fusion of dCas9 to subunits or interaction domains of endogenous co-repressor complexes, such as FOG1[1–45]-dCas9 that interacts with the nucleosome remodeling and deacetylase (NuRD) complex, recruits the NuRD complex to the target sites causing HDAC1/2-mediated H3K27 deacetylation, as well as facilitation of H3K27 tri-methylation through recruitment of the PRC2 complex. (**B**) Schematic of dCas9-FOG1[1–45] fusion proteins. Fusions to the N- and/or C-termini of dCas9 are labeled with [N] and/or [C], respectively. Arrays of two, three and four FOG1[1–45] repeats are fused to dCas9. NLSs, 3XFlag epitope tag and the 15-aa linkers [$(GGS)_5$] are indicated. (**C**) Relative *HER2* mRNA was assessed in HCT116 cells co-transfected with a pool of three sgRNAs targeted to the *HER2* promoter and the indicated dCas9-FOG1[1–45] fusions. Repressive activity was measured relative to Cas9 with no ED (Tukey-test, $*P < 0.05$, $**P < 0.01$, $n = 2$ independent experiments; mean ± SEM). Negative control cells ('−') were transfected with mCherry reporter plasmid instead of dCas9. (**D**) H3K27ac and H3K27me3 enrichments were assessed by ChIP-qPCR at the *HER2* promoter after transfection with a dCas9 with no ED or FOG1[1–45]-dCas9-FOG1[1–45] (Tukey test, *ns*, not significant; $**P < 0.01$; $n = 2$ independent experiments; mean ± SD). ChIP assays using normal rabbit IgG were used as negative controls.

dCas9-FOG1[1-45] is a novel and efficient transcriptional repressor producing H3K27 tri-methylation

As an alternative to the 'direct tethering' of the H3K27me3 methyltransferase Ezh2 (Figure 3A, top), we examined a 'recruitment' paradigm in which an endogenous modifying complex could be recruited by a small peptide attached to dCas9 (Figure 3A, bottom). Recruitment is also the strategy used more frequently by natural transcription factors rather than the direct tethering of enzymes. One such small peptide, the N-terminal 45 residues of Friend Of GATA1 (FOG1), has been associated with tri-methylation of H3K27. It has been shown that repression by the transcription factors GATA1 and GATA2 is dependent on a small conserved domain at the N-terminus of FOG1, which in turn can bind directly to the NuRD complex (31). Recruitment of the NuRD complex causes histone deacetylation at GATA1/2 target sites, followed by recruitment of the PRC2 responsible for methylation of H3K27 (32) (Figure 3A, bottom). However, FOG1 had not previously been used with any of the programmable DNA-binding plat-

forms (ZFPs, TALEs or dCas9). FOG1[1–45] was fused to the N-terminus, the C-terminus, or to both the N- and C-termini of dCas9 (Figure 3B). In contrast to our results for G9A[SET], SUV[SET] and Ezh2[SET], the FOG1[1–45]-dCas9 fusion at the N-terminus did not give rise to a significant decrease in *HER2* transcription in HCT116 cells. However, the C-terminal dCas9-FOG1[1–45] repressed *HER2* expression 3.2-fold (Tuckey HSD test, $P = 0.004$; Figure 3C). In further contrast, the strongest repression was observed with dCas9 containing FOG1[1–45] fusions on both the N- and the C-termini (6.2-fold; Tuckey HSD test, $P = 0.001$; Figure 3C). To evaluate possible synergistic activity of multiple FOG1[1–45] effectors, we created N-terminal dCas9-fusions with arrays of two, three or four FOG1[1–45] repeats separated by 15-aa linkers [$(GGS)_5$] (Supplementary Figure S1). However, these arrays failed to repress as effectively as two FOG1[1–45] domains on either terminus, perhaps due to their reduced expression levels compared to the other FOG1-containing proteins (Supplementary Figure S3B).

Since FOG1[1–45]-dCas9-FOG1[1–45] (also referred to as dCas9-FOG1 [N+C]) showed the strongest repression at the *HER2* target locus, we performed ChIP-qPCR assays to determine enrichment of the histone marks H3K27ac and H3K27me3. While the effect on H3K27ac was not significant (Tukey test, $P = 0.07$), H3K27me3 was increased 5.8-fold (Tukey test, $P < 0.01$; Figure 3D). These data demonstrate that targeting FOG1[1–45] to a specific site in the genome is sufficient to cause H3K27 tri-methylation. Taken together, these findings identify FOG1[1–45]-dCas9-FOG1[1–45] as a novel transcriptional repressor that is associated with H3K27 tri-methylation.

A toolbox of targetable epigenetic regulators demonstrate variable levels of repression at three loci in two cell types

The effect of targeted epigenetic reprograming might be influenced by factors such as epigenetic marks, three-dimensional interactions (e.g. between a promoter and an enhancer, or localization of the DNA region to a sub-nuclear compartment such as a transcriptional factory), and initial expression levels, which may be locus and cell-type dependent. We therefore investigated seven epigenetic modifiers at the *HER2*, *MYC* and *EPCAM* promoters in HCT116 and HEK293T cells. To be more comprehensive in our comparison of epigenetic modifiers having a common dCas9 architecture, we additionally constructed KRAB-dCas9 and DNMT3A-dCas9. The KRAB domain is a commonly used repression domain that like FOG1 acts by recruitment of chromatin modifying complexes. The KRAB domain achieves repression in association with recruitment of the KAP1 co-repressor complex and is associated with H3K9me3 deposition (27). The DNMT3A repression domain extends our toolbox to include targeted *de novo* DNA methylation (16–21). As reported in previous studies (16,17,22,25,48), KRAB-dCas9 caused tri-methylation of H3K9 and DNMT3A-dCas9 induced DNA methylation at the targeted *HER2* promoter (Supplementary Figure S4A and B, respectively). All dCas9 fusions caused some repression of *HER2* expression in HCT116 cells (Tuckey HSD test, $P < 0.05$ and $P < 0.01$; Figure 4A). Ezh2[SET]-dCas9, FOG1[1–45]-dCas9-FOG1[1–45] and DNMT3A-dCas9 produced 2-fold downregulation of *HER2* expression, placing them as somewhat less efficacious than KRAB-dCas9, G9A[SET]-dCas9 and SUV[SET]-dCas9. Differences in *HER2* repression were not correlated with differences in the amount dCas9-fusion protein produced in cells (Supplementary Figure S3C). *HER2* is actively transcribed in HCT116 and HEK293T cells and hence both contain features associated with active promoters. Hallmarks of active promoters are a DNaseI hypersensitive site, acetylation marks (H3K27ac and H3K9ac) as well as methylation marks (H3K4me3 and H3K4me2) (49). In HEK293T cells, only FOG1[1–45]-dCas9-FOG1[1–45] and KRAB-dCas9 were able to downregulate *HER2* expression by more than 2-fold (2.1- and 2.4-fold, respectively, Figure 4B). These data clearly demonstrate that although both cell types have similar epigenetic profiles, epigenetic dCas9-fusions can act in a cell-type dependent manner that at the moment is not predictable.

We next tested dCas9 fusions at different gene promoters. Very modest or no repressive activity was observed at the *MYC* promoter in HCT116 cells (Tuckey HSD test, $P < 0.05$ and $P < 0.01$; Figure 4C), while in HEK293T cells KRAB-dCas9 caused robust downregulation of *MYC* expression (6.2-fold) and DNMT3A-dCas9 and FOG1[1–45]-dCas9-FOG1[1–45] repressed MYC expression 3.7- and 2.3-fold, respectively (Tuckey HSD test, $P < 0.01$; Figure 4D). No significant downregulation was observed with G9A[SET]-dCas9, SUV[SET]-dCas9 and Ezh2[SET]-dCas9. These latter effects may be due to the increased copy number of the *MYC* gene in the HCT116 cell line. Finally, we targeted dCas9 fusions to the *EPCAM* promoter in HCT116 cells (Figure 4E). Surprisingly, only FOG1[1–45]-dCas9-FOG1[1–45] showed significant downregulation (2-fold, Tuckey HSD test, $P < 0.05$). Similar locus and cell-type differences in repression were observed for different configurations of dCas9 with FOG1[1–45] (Supplementary Figure S5). For each target, a pool between three and six sgRNAs was used to target dCas9 fusions to the gene promoter (Figure 4F). Taken together, these data identify FOG1[1–45]-dCas9-FOG1[1–45] and KRAB-dCas9 as the most potent transcriptional repressors at most tested target sites. It is notable that direct fusions of dCas9 with chromatin modifying enzymes are much more susceptible to differences in cell type or target region.

Effector fusions to the catalytically inactive Cpf1 (dCpf1) are not active

To guide different epigenetic effector domains to unique sites within the same or different regulatory elements, it would be helpful to use orthogonal programmable DNA-binding platforms. The RNA-guided endonuclease Cpf1, a type V CRISPR/Cas system, offers a genome editing alternative to the type II CRISPR/Cas9 endonuclease (39,50,51). Unlike Cas9, for which a CRISPR targeting RNA and a *trans*-activating RNA are combined to form a single gRNA, Cpf1 requires only a single CRISPR gRNA (*cr*RNA). *Acidaminococcus* (*As*)Cpf1 efficiently cleaves target DNA adjacent to a short T-rich PAM recognition site (5′-TTTN-3′) whereas *S. pyogenes* (*Sp*)Cas9 requires a G-

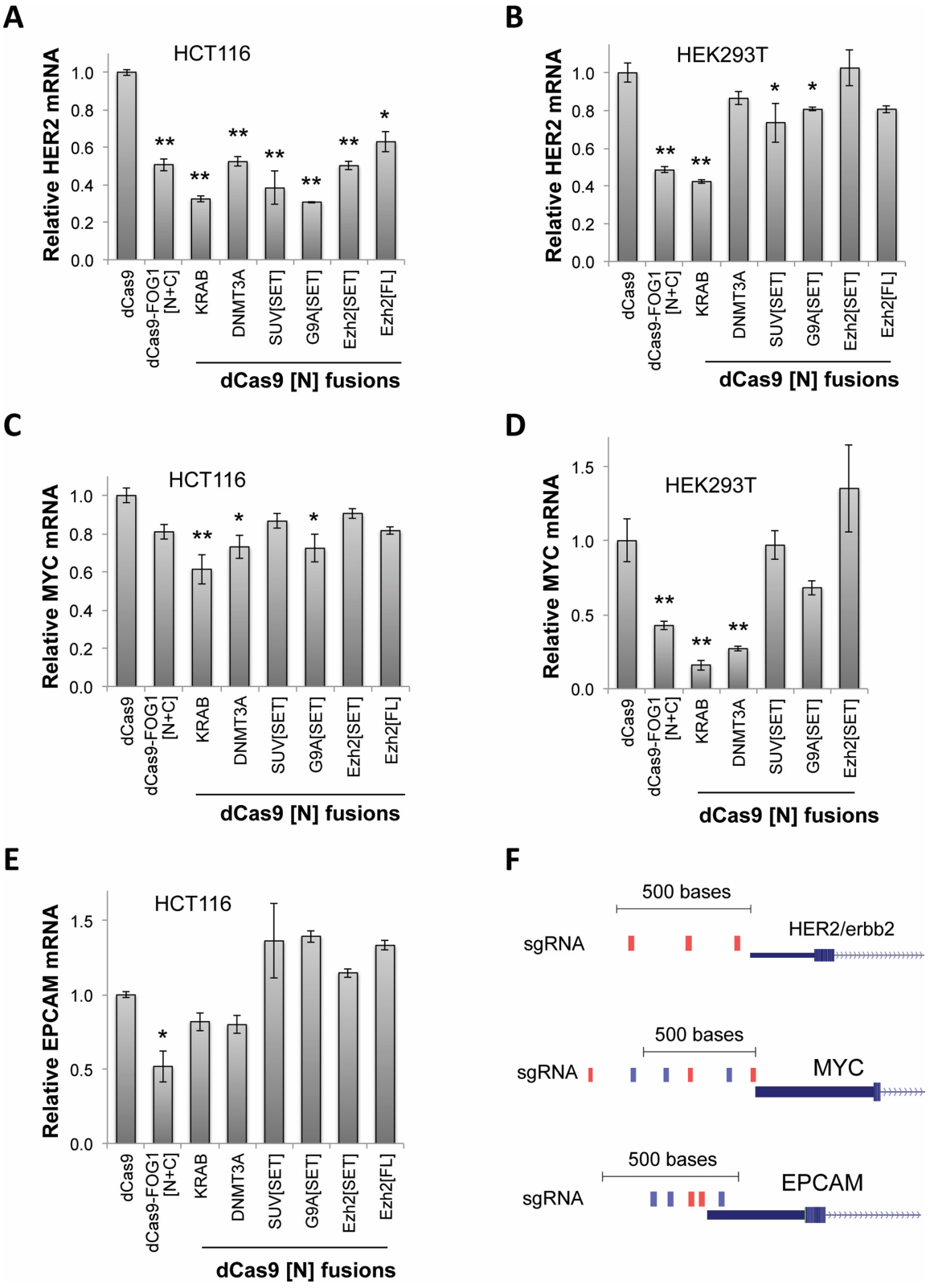

Figure 4. Variable repression mediated by ED-dCas9 epigenetic modifiers at three loci in two cell types. Relative mRNA production in HCT116 (**A**, **C** and **E**) or HEK293T (**B** and **D**) cells co-transfected with a pool of sgRNAs targeted to the *HER2* (A and B), MYC (C and D) or *EPCAM* (E) promoter with the indicated dCas9 fusions. Expression data are shown in comparison to cells transfected by dCas9 with no ED (Tukey-test, $*P < 0.05$, $**P < 0.01$, (A and E) $n = 2$ and (B–D) $n = 3$ independent experiments; mean ± SEM). (**F**) The positions of sgRNAs are indicated for each promoter.

rich PAM site (5′-NGG-3′) hence broadening in principle the number and diversity of target sites in the genome that are accessible to precise gene editing. Since our goal is to develop tools that target the epigenome, but do not cleave the target DNA, we used a catalytically 'dead' Cpf1 [D908A] (dCpf1; Figure 5A). To confirm loss of cleavage activity of dCpf1, we performed SSA assays using a mCherry reporter system (52). The mCherry gene was split into two inactive fragments containing overlapping homologies with a *HER2* promoter target site between them (Supplementary Figure S2A). In cells, cleavage at the *HER2* site will initiate single strand annealing and generate an active mCherry gene, causing cells to accumulate fluorescent mCherry protein. Co-transfection of wild-type *As*Cpf1 with a *HER2* crRNA resulted in red fluorescence; however, as expected, no red fluorescence was observed when catalytically inactive dCpf1 was used (Supplementary Figure S2B). We then constructed KRAB-dCpf1, EZH2[SET]-dCpf1, SUV[SET]-dCpf1, DNMT3A-dCpf1, dCpf1-DNMT3A and FOG1[1–45]-dCpf1-FOG1[1–45] (Figure 5A), and tested their repressive activity at the *HER2* promoter in HCT116 cells using three crRNAs simultaneously (Figure 5B). Surprisingly, none of the dCpf1 fusions were able to repress transcription of *HER2,* while a dCas9 version of FOG1[1–45]-dCas9-FOG1[1–45] demonstrated the expected repression (Figure 5C). We then performed ChIP assays to confirm that creating the catalytic mutant dCpf1 did not interfere with the ability of dCpf1 to bind to its target site. dCas9 binding to the *HER2* promoter was used as the gold standard and was targeted to the *HER2* promoter either by one sgRNA (sgRNA2) or a pool of three sgRNAs (Figure 1B). Similarly, dCpf1 was targeted to the *HER2* promoter with each individual crRNA or a pool of all three crRNAs (Figure 5B). ChIP enrichments of dCas9 or dCpf1 were indistinguishable whether one or a pool of sgRNAs or crRNAs was used (Tuckey HSD test, $P = 0.001$, Figure 5D). After this important preliminary finding, we next assessed if addition of effector domains destabilizes dCpf1 binding to the target site. We assessed ChIP enrichment for FOG1[1–45]-dCpf1-FOG1[1–45] and KRAB-dCpf1. Binding of FOG1[1–45]-dCpf1-FOG1[1–45] and KRAB-dCpf1 were not significantly different when compared to dCpf1 alone (Tuckey HSD test, Figure 5E). These data suggest major differences between the dCas9 and dCpf1 scaffolds and mode of action when bound to the target site.

EZH2[FL]-dCas9 and DNMT3A-dCas9 establish persistent repression, while FOG1[1-45]-dCas9-FOG1[1-45] and KRAB-dCas9 drive robust transient repression

We next tested if transient expression of dCas9 fusion proteins could cause persistent *HER2* gene repression and if combinations of dCas9 fusion proteins could increase transient and/or persistent downregulation of *HER2* expression. Transient repression was measured four days after transfection under puromycin selection to enrich for transfected cells, while the persistent effect was determined after cells were grown for an additional 10 days in puromycin free media (Figure 6A). This procedure enriched for transfected cells but avoided selection of stably integrated epigenetic modifier expression plasmids, ensuring that persistent repression would be due to altered epigenetic states (data not shown). Repressive activity was determined for DNMT3A fused to the N- or C-terminus of dCas9 (DNMT3A-dCas9 and dCas9-DNMT3A, respectively). DNMT3A-dCas9 and dCas9-DNMT3A caused only modest downregulation of 1.5- and 1.4-fold, respectively; however, the repression was persistent over 10 days (Figure 6B). In contrast, KRAB-dCas9 achieved a 5-fold downregulation of *HER2*, but expression was completely restored 10 days later. KRAB-dCas9 dominated transient repression, and addition of DNMT3A-dCas9, dCas9-DNMT3A or overexpressed DNMT3L neither increased repression nor persistence (Figure 6B). We then assessed the contributions of the two H3K27me3 producing fusions, FOG1[1–45]-dCas9-FOG1[1–45] and Ezh2[FL]-dCas9, on the level and persistence of repression. FOG1[1–45]-dCas9-FOG1[1–45] downregulated *HER2* expression 2-fold, but *HER2* expression reverted to normal after 10 days (Figure 6C). Addition of DNMT3A-dCas9 and overexpression of DNMT3L improved the persistence of downregulation; however, the same expression level and persistence was achieved by DNMT3A-dCas9 alone. Ezh2[FL]-dCas9 was also able to cause a level of *HER2* downregulation similar to DNMT3A-dCas9. The level and persistence of repression by Ezh2[FL]-dCas9 was further enhanced by addition of DNMT3A-dCas9 and overexpressed DNMT3L (Tuckey HSD test, $P = 0.02$; Figure 6C). Taken together, FOG1[1–45]-dCas9-FOG1[1–45] and KRAB-dCas9 produce a transient but strong repression, while Ezh2[FL]-dCas9 and DNMT3A-dCas9 drive persistent but more modest repression.

DISCUSSION

Precise control of transcription and epigenetics at a defined genomic locus provides an ability to dissect links between the two processes in a way not formerly possible. In this study, we generated a set of epigenome editing tools to deposit epigenetic marks typically associated with a repressed chromatin state, including DNA methylation and histone methylation (both H3K9me3 and H3K27me3). Our epigenetic fusions of dCas9 with HMT complement recently described epigenetic editing tools, which have been mostly focused on DNA methylation and demethylation (16–21). Our study made use of a common dCas9 architecture and assayed a broad assortment of epigenetic effector domains at three loci in two cell types. Direct enzyme tethering versus co-repressor recruitment strategies were also examined.

The major finding of this study was that transcriptional repression was independent of deposition of the expected repressive chromatin mark. While dCas9 alone did not produce repression, evidence from Ezh2[SET]-dCas9 catalytic mutants (Figure 2F) suggested that some amount of repression was due to a non-catalytic activity of the effector domains. This activity could occur by a mechanism such as steric hindrance of endogenous activation factors, or by an interaction with other components of repression complexes. A similar observation was recently reported by Wysocka *et al.*, in which the methyltransferase catalytic activity of MII3/4 proteins was dispensable for transcription, but the proteins themselves were required due to their protein bind-

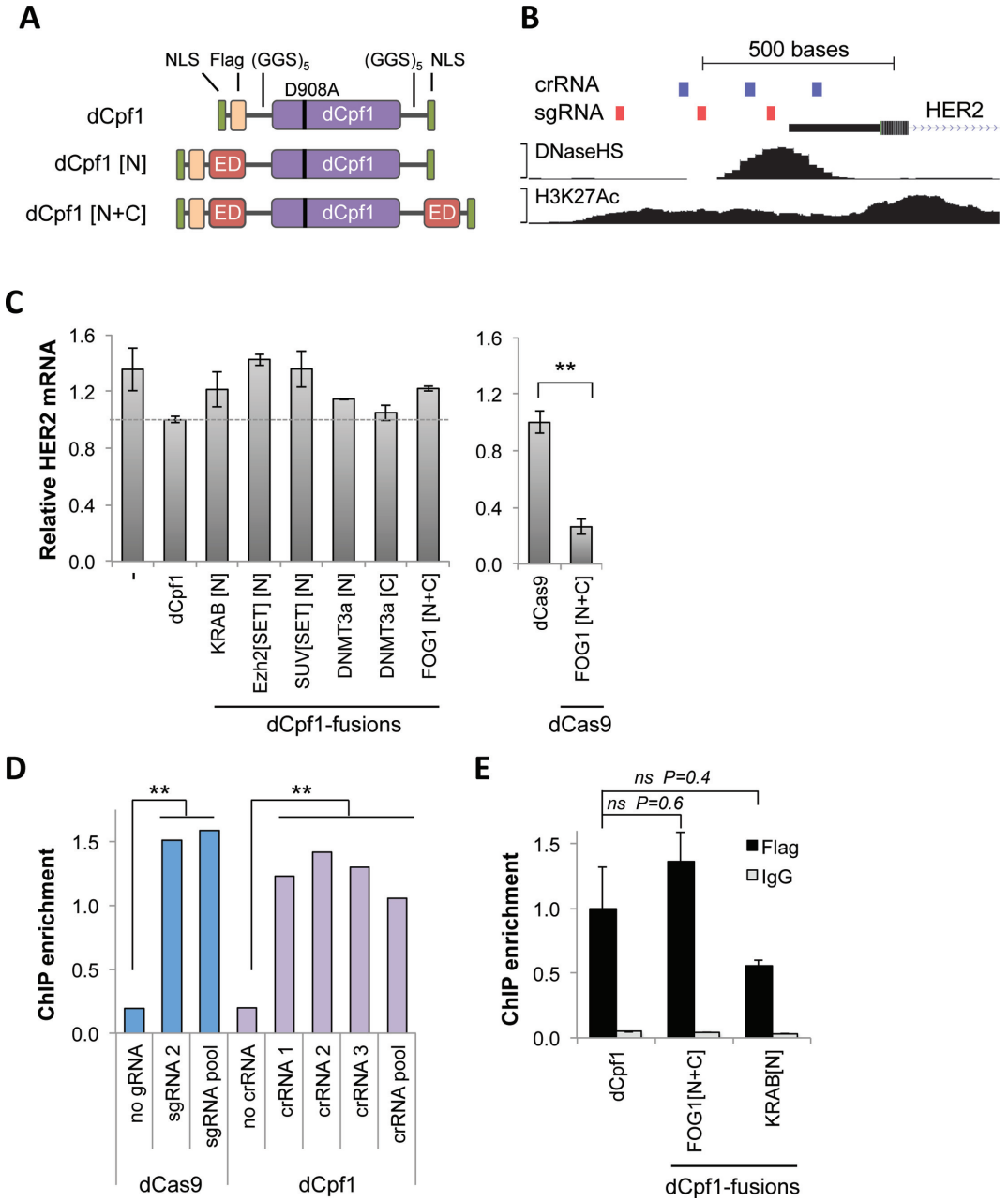

Figure 5. dCpf1-epigenetic fusions do not repress *HER2* gene expression. (**A**) Schematic of dCpf1-fusions with ED. Catalytically inactive *As*Cpf1 contains nuclease-inactivating mutation D908A (dCpf1). (**B**) UCSC genome browser graphic showing *HER2* target regions of sgRNAs containing the 5′-NGG-3′ PAM required by dCas9, and crRNA target sites flanked by the 5′-NTTT-3′ PAM required by dCpf1. HCT116 ENCODE tracks for DNase Hypersensitivity (DNase HS) and H3K27ac binding are shown. (**C**) Abundance of *HER2* mRNA was measured after co-transfection of HCT116 cells with a pool of three crRNAs with the indicated dCpf1-ED fusions. No significant repression was observed compared to a dCpf1 with no ED. Negative control cells ('−') were transfected with mCherry reporter plasmid instead of dCpf1. As a positive control, repression was assessed after co-transfection of dCas9 with no ED or FOG1[1–45]-dCas9-FOG1[1–45] and three sgRNAs (Tukey-test, $P < 0.01$, $n = 2$ independent experiments; mean ± SEM). (**D**) dCas9 and dCpf1 enrichments were assessed by ChIP-qPCR at the *HER2* promoter after transfection with a dCas9 or dCpf1 with no ED and the indicated sgRNA or crRNA. Statistical significance was analyzed by combining enrichments in the absence of a sgRNA or crRNA ($n = 2$) and compared to dCas9 with sgRNA2 and sgRNA pool data ($n = 2$) and with combined dCpf1/crRNA data ($n = 4$) (Tukey test, $P = 0.001$). (**E**) dCpf1 enrichments were assayed after transfection with the indicated dCpf1 with no ED or the indicated fusion, and the three crRNAs (*ns*, not significant; $n = 2$ independent experiments; mean ± SEM). ChIP assays using normal rabbit IgG as negative controls are shown.

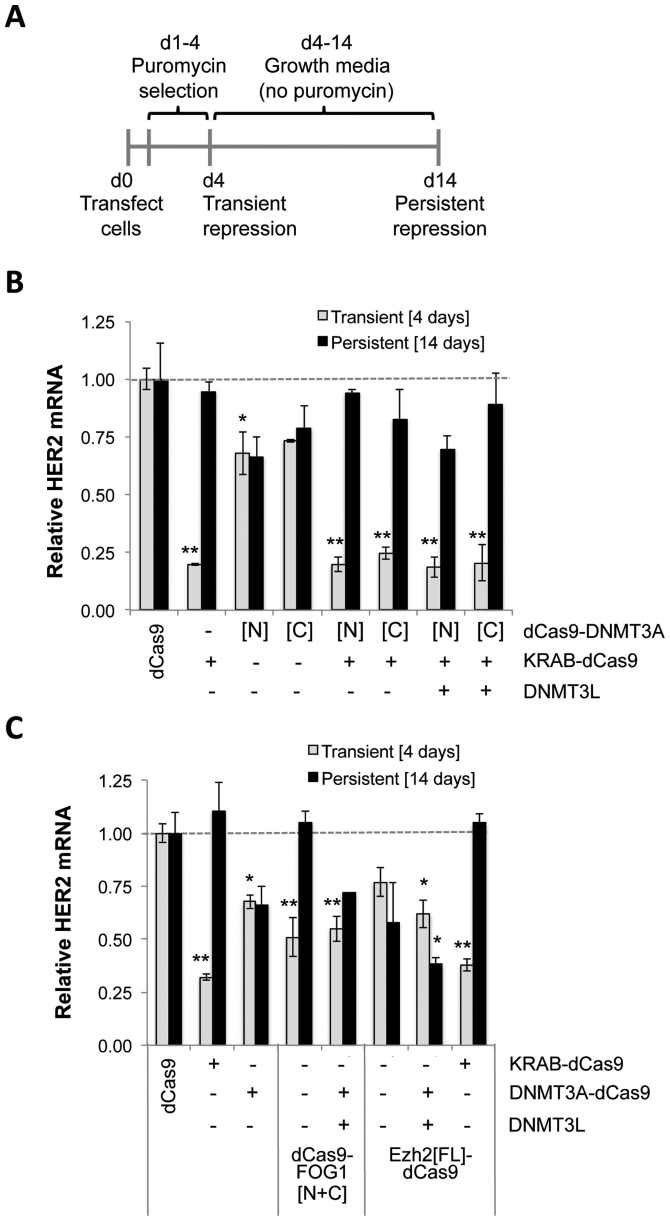

Figure 6. Combinations of epigenetic modifiers can achieve long-term gene repression. (**A**) Schematic of experimental design for transient transfection assays with partial puromycin enrichment. (**B**) Relative *HER2* mRNA production in HCT116 cells co-transfected with a pool of three sgRNAs targeted to the *HER2* gene promoter and combinations of N- or C-terminal DNMT3A-dCas9 fusions, KRAB-dCas9 and DNMT3L. (**C**) Relative *HER2* mRNA production using combinations of N-terminal DNMT3A-dCas9, KRAB-dCas9, DNMT3L, FOG1[1–45]-dCas9-FOG1[1–45] and Ezh2[FL]-dCas9. Expression data are shown in comparison to cells transfected by dCas9 with no ED. Statistical significance was analyzed for the transient effect by comparing dCas9 fusions to dCas9 without an effector domain after 4 days, while significance of persistent repression was calculated by comparing dCas9 fusions to dCas9 without ED after 14 days (Tukey-test, $*P < 0.05$, $**P < 0.01$, $n = 2$ independent experiments; mean ± SEM).

ing interactions with other factors (53). However, several of our tested domains were able to deposit their expected chromatin marks, but the chromatin marks appeared to produce no additional gene repression (Figures 1E and 2C). These data therefore demonstrate that deposition of so-called epigenetic repressive histone marks is not sufficient to cause transcriptional repression.

The KRAB domain achieves repression in association with recruitment of the KAP1 co-repressor complex which contains the histone methyltransferase SETDB1, initiating tri-methylation of H3K9 (27). The HMT SUV39H1 and G9A have also been associated with H3K9me3. In contrast, the two new functional domains introduced in this study, Ezh2 and FOG1, are both associated with H3K27me3. Ezh2 is a catalytic component of the PRC2 complex responsible for H3K27me2/3. GATA-1 and its cofactor FOG1 bind to their genomic targets and repress gene expression through recruitment of the NuRD complex. In biochemical studies, FOG1[1–45] has been shown to interact with several proteins that are part of the NuRD complex, such as histone deacetylases HDAC1/2, CHD4, MBD2/3 as well as MTA-1 and MTA-2 (31,54). NuRD-mediated deacetylation of H3K27 in turn allows for H3K27 tri-methylation by the PRC2 complex (32,55). In our studies, FOG1[1–45]-dCas9-FOG1[1–45] showed the strongest repression at the *HER2* target locus compared to any of the other effector domains tested, and also provided strong deposition of H3K27me3. These findings present FOG1[1–45]-dCas9-FOG1[1–45] as a newly described, highly efficient transcriptional repressor associated with H3K27 tri-methylation.

The catalytic domains for Ezh2, G9A and SUV39H1 have been mapped to their C-terminal SET domains (30,47). G9A[SET]-dCas9 was able to deposit H3K9me3 and a full-length Ezh2[FL]-dCas9 was able to deposit H3K27me3, however SUV[SET]-dCas9 and Ezh2[SET]-dCas9 were not able to deposit their expected marks. These observations indicate that the SET domains of SUV and Ezh2 are not sufficient for H3K9 or H3K27 tri-methylation but that other parts of the full-length proteins may also be required for histone methylation, at least in the context of dCas9 fusion proteins. Perhaps this is not unexpected as other domains of the Ezh2 protein are important for interaction with members of the PRC2 complex, such as Suz12 and EED, as well as other epigenetic modifying enzymes such as DNA methyltransferases (56,57). We also note that SUV39H1 has Glu-repeat, Cys-repeat, Ankyrin and Chomodomain domains upstream of the SET domain (30), which may be important for catalytic (epigenetic writing) activity.

Two strategies can be used to epigenetically repress a specific endogenous gene: (i) direct targeting of a chromatin modifying enzyme itself to DNA or (ii) recruitment of a chromatin remodeling complex that contains several enzymatic capabilities. Although in nature, epigenetic enzymes are rarely attached to DNA-binding domains directly, our results using the enzymatic domains of EZH2, SUV and G9A, as well as those of several other studies (16,17,22–24), suggest that the first strategy can be effective experimentally. Our novel transcriptional repressor consisting of dCas9 fused to FOG1[1–45] is an example of the alternative repression strategy based on recruitment of a co-repressor,

as opposed to fusion of an enzymatic component to dCas9. In addition to any functional advantages (e.g. improved target-gene repression), the use of a short peptide is less likely to interfere with endogenous regulatory factors at the promoter than the direct tethering of large enzymes. It also provides an opportunity to increase its effect by multiplexing the short interaction peptides, such as is frequently done with the herpes simplex VP16 activation domain to produce the more effective VP64 (58,59). However, our data demonstrate that some configurations of arrayed repeats can actually reduce protein expression, which could have accounted for the reduced repression of our tandem FOG1 arrays. Future designs of arrayed domains should consider such effects.

Our toolbox of epigenetic editors was found to have locus and cell-type dependent effects on transcriptional repression, ranging from nearly no significant repression by any factor at the MYC promoter in HCT116 cells to nearly 10-fold repression by one factor at MYC in HEK293T cells. HCT116 is a colon cancer cell line that contains amplified regions in the genome resulting in additional copies of affected genes. The *MYC* gene is located in such an amplified region in HCT116 cells and is thus present in three copies, while there are two copies of the *EPCAM* and *HER2* genes. We cannot conclude whether the lack of repression is a cell-type specific phenomenon per se or if it is more difficult to achieve repression in the presence of additional MYC gene copies. The effect of targeted epigenetic reprograming might also be influenced by existing epigenetic marks, three-dimensional interactions and initial expression levels, as well as other factors. Additional studies will be required to understand the molecular basis for the observed locus and cell-type dependent effects.

Surprisingly, none of the dCpf1-effector domain fusions had an effect on gene expression, despite evidence of binding to the DNA target sites. In contrast to the G-rich PAM site (5′-NGG-3′) required by the *S. pyogenes* (*Sp*)Cas9, *Acidaminococcus sp. BV3L6* (*As)*Cpf1 is an RNA-guided nuclease that can use a short T-rich PAM recognition site (5′-TTTN-3′) (39,50). Targeting both T-rich as well as C-rich chromatin regions would broaden the number of target sites in the genome that are accessible to epigenetic editing, and would have been a useful orthogonal platform for targeting different effectors to the same gene or simultaneously activating and repressing different genes in the same cell. Notably, there have not been any reports of dCpf1 based activators (e.g. VP64) or repressors (e.g. KRAB) in mammalian cells. In *Arabidopsis*, fusions of catalytic inactive Cpf1 (As-Cpf1[D908A] and LbCpf1 [D832A]) with three copies of the SRDX repressor domain were used to repress a non-coding RNA (60). Unfortunately, the dCpf1 used here was not suitable for targeted transcriptional regulation. We also note that Ezh2[SET]-dCas9 was observed to produce gene repression through a non-catalytic process such as steric hindrance (Figure 2F), but no such repression was observed when Ezh2[SET] was tethered to dCpf1. These observations suggest unexpected differences between dCas9 and dCpf1 platforms. However, it is possible that dCpf1 fusions will be successful with different features or at different genomic loci.

In addition to orthogonal gene regulation, epigenetic editing holds the great potential for persistent changes in gene expression without altering genetic sequence. In nature, H3K9me3 and H3K27me3 are often associated with silenced states of genes and other elements that are stable over the lifetime of an individual. However, far less is known about the transitions between active and silenced states. It has been shown that targeting DNMT3A to a gene promoter can be sufficient to achieve persistent gene silencing (16,61,62). Although targeting DNMT3A results in methylation at the target site, we and others have found the down-regulation of gene expression is often modest (17,48). In certain cell types, targeting KRAB and DNMT3L in addition to DNMT3A was required for persistent gene silencing (61). However, KRAB-dCas9 had no effect on promoting persistent silencing in our study, while the dCas9 fusion with the epigenetic writer of H3K27me3 (Ezh2[FL]) facilitated persistence.

Targeting epigenetic modifying enzymes allowed us to interrogate the causal relationship between the epigenetic marks and gene expression at the target site. Surprisingly, we found that deposition of the expected histone modification was not sufficient for transcriptional repression. This result is similar to our previous finding that the level of H3K27ac at an enhancer region is not correlated with the activity of that enhancer in its endogenous genomic context (63). Our current study has expanded the list of tools available for epigenetic editing (6) to include new targeted tools to deposit H3K27me3. However, almost all targeted epigenetic modifiers reported to date have fallen well short of producing the dramatic differences in the level of gene repression observed in natural epigenetic states. Before we can truly gain predictable epigenetic control of endogenous gene expression, several features need to be better understood: the length of the region requiring epigenetic modification, the persistence of the modified marks, the persistence of machinery for reinforcing the marks, the effect of multiple types of marks in a region and of course the relationship between epigenetic marks and gene expression. These issues will likely be the inspiration for many future studies in the vibrant nascent field of epigenome editing.

SUPPLEMENTARY DATA

Supplementary Data are available at NAR Online.

ACKNOWLEDGEMENTS

We thank Marianne Rots for generously providing G9A, SUV39H1 and DNMT3A cDNA and Fred Chedin for contributing pCDNA-DNMT3L. We also thank Joshua Meckler for advice and providing the dCas9 plasmid backbone, and Paul Knoepfler for a careful reading of the manuscript. Author contributions: H.O., P.J.F. and D.J.S. conceived the study and designed the experiments. J.P.M. conceived of the FOG1 co-repressor recruitment peptide. C.R. conceived the dCpf1 study and designed the dCPf1 experiments. H.O., C.R. and J.H. contributed to plasmid construction. H.O., C.R., C.M.N., A.A.P., J.H. and V.L. performed experiments. H.O. and C.R. analyzed the data. H.O. and D.J.S. wrote the manuscript. All authors contributed to the editing of the manuscript and approved its final version.

FUNDING

National Institutes of Health (NIH) [CA204563 to D.J.S.]; Australian Research Council [DP160104106 to J.P.M]; Foundation for Angelman Syndrome Therapeutics [to D.J.S]. The open access publication charge for this paper has been waived by Oxford University Press - *NAR* Editorial Board members are entitled to one free paper per year in recognition of their work on behalf of the journal.
Conflict of interest statement. None declared.

REFERENCES

1. Jenuwein,T. and Allis,C.D. (2001) Translating the histone code. *Science*, **293**, 1074–1080.
2. Berger,S.L. (2007) The complex language of chromatin regulation during transcription. *Nature*, **447**, 407–412.
3. Consortium,E.P., Bernstein,B.E., Birney,E., Dunham,I., Green,E.D., Gunter,C. and Snyder,M. (2012) An integrated encyclopedia of DNA elements in the human genome. *Nature*, **489**, 57–74.
4. Roadmap Epigenomics,C., Kundaje,A., Meuleman,W., Ernst,J., Bilenky,M., Yen,A., Heravi-Moussavi,A., Kheradpour,P., Zhang,Z., Wang,J. *et al.* (2015) Integrative analysis of 111 reference human epigenomes. *Nature*, **518**, 317–330.
5. You,J.S., Kelly,T.K., De Carvalho,D.D., Taberlay,P.C., Liang,G. and Jones,P.A. (2011) OCT4 establishes and maintains nucleosome-depleted regions that provide additional layers of epigenetic regulation of its target genes. *Proc. Natl. Acad. Sci. U.S.A.*, **108**, 14497–14502.
6. Stricker,S.H., Koferle,A. and Beck,S. (2017) From profiles to function in epigenomics. *Nat. Rev. Genet.*, **18**, 51–66.
7. Segal,D.J. and Meckler,J.F. (2013) Genome engineering at the dawn of the golden age. *Annu. Rev. Genomics Hum. Genet.*, **14**, 135–158.
8. Falahi,F., Sgro,A. and Blancafort,P. (2015) Epigenome engineering in cancer: fairytale or a realistic path to the clinic? *Front. Oncol.*, **5**, 22.
9. Hilton,I.B. and Gersbach,C.A. (2015) Enabling functional genomics with genome engineering. *Genome Res.*, **25**, 1442–1455.
10. Jinek,M., Chylinski,K., Fonfara,I., Hauer,M., Doudna,J.A. and Charpentier,E. (2012) A programmable dual-RNA-guided DNA endonuclease in adaptive bacterial immunity. *Science*, **337**, 816–821.
11. Jinek,M. (2012) A programmable dual-RNA-guided DNA endonuclease in adaptive bacterial immunity. *Science*, **337**, 816–821.
12. Sternberg,S.H., Redding,S., Jinek,M., Greene,E.C. and Doudna,J.A. (2014) DNA interrogation by the CRISPR RNA-guided endonuclease Cas9. *Nature*, **507**, 62–67.
13. Perez-Pinera,P., Kocak,D.D., Vockley,C.M., Adler,A.F., Kabadi,A.M., Polstein,L.R., Thakore,P.I., Glass,K.A., Ousterout,D.G., Leong,K.W. *et al.* (2013) RNA-guided gene activation by CRISPR-Cas9-based transcription factors. *Nat. Methods*, **10**, 973–976.
14. Maeder,M.L., Linder,S.J., Cascio,V.M., Fu,Y., Ho,Q.H. and Joung,J.K. (2013) CRISPR RNA-guided activation of endogenous human genes. *Nat. Methods*, **10**, 977–979.
15. Gilbert,L.A., Larson,M.H., Morsut,L., Liu,Z., Brar,G.A., Torres,S.E., Stern-Ginossar,N., Brandman,O., Whitehead,E.H., Doudna,J.A. *et al.* (2013) CRISPR-mediated modular RNA-guided regulation of transcription in eukaryotes. *Cell*, **154**, 442–451.
16. Vojta,A., Dobrinic,P., Tadic,V., Bockor,L., Korac,P., Julg,B., Klasic,M. and Zoldos,V. (2016) Repurposing the CRISPR-Cas9 system for targeted DNA methylation. *Nucleic Acids Res.*, **44**, 5615–5628.
17. McDonald,J.I., Celik,H., Rois,L.E., Fishberger,G., Fowler,T., Rees,R., Kramer,A., Martens,A., Edwards,J.R. and Challen,G.A. (2016) Reprogrammable CRISPR/Cas9-based system for inducing site-specific DNA methylation. *Biol. Open*, **5**, 866–874.
18. Xu,X., Tao,Y., Gao,X., Zhang,L., Li,X., Zou,W., Ruan,K., Wang,F., Xu,G.L. and Hu,R. (2016) A CRISPR-based approach for targeted DNA demethylation. *Cell Discov.*, **2**, 16009.
19. Choudhury,S.R., Cui,Y., Lubecka,K., Stefanska,B. and Irudayaraj,J. (2016) CRISPR-dCas9 mediated TET1 targeting for selective DNA demethylation at BRCA1 promoter. *Oncotarget*.**7**, 46545–46556.
20. Morita,S., Noguchi,H., Horii,T., Nakabayashi,K., Kimura,M., Okamura,K., Sakai,A., Nakashima,H., Hata,K., Nakashima,K. *et al.* (2016) Targeted DNA demethylation in vivo using dCas9-peptide repeat and scFv-TET1 catalytic domain fusions. *Nat. Biotechnol.*, **34**, 1060–1065.
21. Liu,X.S., Wu,H., Ji,X., Stelzer,Y., Wu,X., Czauderna,S., Shu,J., Dadon,D., Young,R.A. and Jaenisch,R. (2016) Editing DNA Methylation in the Mammalian Genome. *Cell*, **167**, 233–247.
22. Kearns,N.A., Pham,H., Tabak,B., Genga,R.M., Silverstein,N.J., Garber,M. and Maehr,R. (2015) Functional annotation of native enhancers with a Cas9-histone demethylase fusion. *Nat. Methods*, **12**, 401–403.
23. Hilton,I.B., D'Ippolito,A.M., Vockley,C.M., Thakore,P.I., Crawford,G.E., Reddy,T.E. and Gersbach,C.A. (2015) Epigenome editing by a CRISPR-Cas9-based acetyltransferase activates genes from promoters and enhancers. *Nat. Biotechnol.*, **33**, 510–517.
24. Cano-Rodriguez,D., Gjaltema,R.A., Jilderda,L.J., Jellema,P., Dokter-Fokkens,J., Ruiters,M.H. and Rots,M.G. (2016) Writing of H3K4Me3 overcomes epigenetic silencing in a sustained but context-dependent manner. *Nat. Commun.*, **7**, 12284.
25. Thakore,P.I., D'Ippolito,A.M., Song,L., Safi,A., Shivakumar,N.K., Kabadi,A.M., Reddy,T.E., Crawford,G.E. and Gersbach,C.A. (2015) Highly specific epigenome editing by CRISPR-Cas9 repressors for silencing of distal regulatory elements. *Nat. Methods*, **12**, 1143–1149.
26. Schultz,D.C., Ayyanathan,K., Negorev,D., Maul,G.G. and Rauscher,F.J. 3rd (2002) SETDB1: a novel KAP-1-associated histone H3, lysine 9-specific methyltransferase that contributes to HP1-mediated silencing of euchromatic genes by KRAB zinc-finger proteins. *Genes Dev.*, **16**, 919–932.
27. Feschotte,C. and Gilbert,C. (2012) Endogenous viruses: insights into viral evolution and impact on host biology. *Nat. Rev. Genet.*, **13**, 283–296.
28. Schultz,D.C., Friedman,J.R. and Rauscher,F.J. 3rd (2001) Targeting histone deacetylase complexes via KRAB-zinc finger proteins: the PHD and bromodomains of KAP-1 form a cooperative unit that recruits a novel isoform of the Mi-2alpha subunit of NuRD. *Genes Dev.*, **15**, 428–443.
29. Falahi,F., Huisman,C., Kazemier,H.G., van der Vlies,P., Kok,K., Hospers,G.A. and Rots,M.G. (2013) Towards sustained silencing of HER2/neu in cancer by epigenetic editing. *Mol. Cancer Res.*, **11**, 1029–1039.
30. Dillon,S.C., Zhang,X., Trievel,R.C. and Cheng,X. (2005) The SET-domain protein superfamily: protein lysine methyltransferases. *Genome Biol.*, **6**, 227.
31. Hong,W., Nakazawa,M., Chen,Y.Y., Kori,R., Vakoc,C.R., Rakowski,C. and Blobel,G.A. (2005) FOG-1 recruits the NuRD repressor complex to mediate transcriptional repression by GATA-1. *EMBO J.*, **24**, 2367–2378.
32. Ross,J., Mavoungou,L., Bresnick,E.H. and Milot,E. (2012) GATA-1 utilizes Ikaros and polycomb repressive complex 2 to suppress Hes1 and to promote erythropoiesis. *Mol. Cell. Biol.*, **32**, 3624–3638.
33. O'Geen,H., Henry,I.M., Bhakta,M.S., Meckler,J.F. and Segal,D.J. (2015) A genome-wide analysis of Cas9 binding specificity using ChIP-seq and targeted sequence capture. *Nucleic Acids Res.*, **43**, 3389–3404.
34. Rivenbark,A.G., Stolzenburg,S., Beltran,A.S., Yuan,X., Rots,M.G., Strahl,B.D. and Blancafort,P. (2012) Epigenetic reprogramming of cancer cells via targeted DNA methylation. *Epigenetics*, **7**, 350–360.
35. Chedin,F., Lieber,M.R. and Hsieh,C.L. (2002) The DNA methyltransferase-like protein DNMT3L stimulates de novo methylation by Dnmt3a. *Proc. Natl. Acad. Sci. U.S.A.*, **99**, 16916–16921.
36. Mali,P., Yang,L., Esvelt,K.M., Aach,J., Guell,M., DiCarlo,J.E., Norville,J.E. and Church,G.M. (2013) RNA-guided human genome engineering via Cas9. *Science*, **339**, 823–826.
37. Montague,T.G., Cruz,J.M., Gagnon,J.A., Church,G.M. and Valen,E. (2014) CHOPCHOP: a CRISPR/Cas9 and TALEN web tool for genome editing. *Nucleic Acids Res.*, **42**, W401–W407.
38. Yamano,T., Nishimasu,H., Zetsche,B., Hirano,H., Slaymaker,I.M., Li,Y., Fedorova,I., Nakane,T., Makarova,K.S., Koonin,E.V. *et al.* (2016) Crystal structure of Cpf1 in complex with guide RNA and target DNA. *Cell*, **165**, 949–962.
39. Zetsche,B., Gootenberg,J.S., Abudayyeh,O.O., Slaymaker,I.M., Makarova,K.S., Essletzbichler,P., Volz,S.E., Joung,J., van der Oost,J.,

Regev,A. *et al.* (2015) Cpf1 is a single RNA-guided endonuclease of a class 2 CRISPR-Cas system. *Cell*, **163**, 759–771.
40. Kim,D., Kim,J., Hur,J.K., Been,K.W., Yoon,S.H. and Kim,J.S. (2016) Genome-wide analysis reveals specificities of Cpf1 endonucleases in human cells. *Nat. Biotechnol.*, **34**, 863–868.
41. O'Geen,H., Frietze,S. and Farnham,P.J. (2010) Using ChIP-seq technology to identify targets of zinc finger transcription factors. *Methods Mol. Biol.*, **649**, 437–455.
42. Li,L.C. and Dahiya,R. (2002) MethPrimer: designing primers for methylation PCRs. *Bioinformatics*, **18**, 1427–1431.
43. Ren,C., Xu,K., Liu,Z., Shen,J., Han,F., Chen,Z. and Zhang,Z. (2015) Dual-reporter surrogate systems for efficient enrichment of genetically modified cells. *Cell. Mol. Life Sci.*, **72**, 2763–2772.
44. Anders,C., Niewoehner,O., Duerst,A. and Jinek,M. (2014) Structural basis of PAM-dependent target DNA recognition by the Cas9 endonuclease. *Nature*, **513**, 569–573.
45. O'Geen,H., Squazzo,S.L., Iyengar,S., Blahnik,K., Rinn,J.L., Chang,H.Y., Green,R. and Farnham,P.J. (2007) Genome-wide analysis of KAP1 binding suggests autoregulation of KRAB-ZNFs. *PLoS Genet.*, **3**, e89.
46. Jamieson,K., Wiles,E.T., McNaught,K.J., Sidoli,S., Leggett,N., Shao,Y., Garcia,B.A. and Selker,E.U. (2016) Loss of HP1 causes depletion of H3K27me3 from facultative heterochromatin and gain of H3K27me2 at constitutive heterochromatin. *Genome Res.*, **26**, 97–107.
47. Trievel,R.C., Beach,B.M., Dirk,L.M., Houtz,R.L. and Hurley,J.H. (2002) Structure and catalytic mechanism of a SET domain protein methyltransferase. *Cell*, **111**, 91–103.
48. Stepper,P., Kungulovski,G., Jurkowska,R.Z., Chandra,T., Krueger,F., Reinhardt,R., Reik,W., Jeltsch,A. and Jurkowski,T.P. (2016) Efficient targeted DNA methylation with chimeric dCas9-Dnmt3a-Dnmt3L methyltransferase. *Nucleic Acids Res.* , **45**, 1703–1713.
49. Consortium,E.P. (2012) An integrated encyclopedia of DNA elements in the human genome. *Nature*, **489**, 57–74.
50. Zetsche,B., Heidenreich,M., Mohanraju,P., Fedorova,I., Kneppers,J., DeGennaro,E.M., Winblad,N., Choudhury,S.R., Abudayyeh,O.O., Gootenberg,J.S. *et al.* (2016) Multiplex gene editing by CRISPR-Cpf1 using a single crRNA array. *Nat. Biotechnol.*, **35**, 31–34.
51. Kim,H.K., Song,M., Lee,J., Menon,A.V., Jung,S., Kang,Y.M., Choi,J.W., Woo,E., Koh,H.C., Nam,J.W. *et al.* (2017) In vivo high-throughput profiling of CRISPR-Cpf1 activity. *Nat. Methods*, **14**, 153–159.
52. Szczepek,M., Brondani,V., Buchel,J., Serrano,L., Segal,D.J. and Cathomen,T. (2007) Structure-based redesign of the dimerization interface reduces the toxicity of zinc-finger nucleases. *Nat. Biotechnol.*, **25**, 786–793.
53. Dorighi,K.M., Swigut,T., Henriques,T., Bhanu,N.V., Scruggs,B.S., Nady,N., Still,C.D. 2nd, Garcia,B.A., Adelman,K. and Wysocka,J. (2017) Mll3 and Mll4 facilitate enhancer RNA synthesis and transcription from promoters independently of H3K4 monomethylation. *Mol. Cell*, **66**, 568–576.
54. Saathoff,H., Brofelth,M., Trinh,A., Parker,B.L., Ryan,D.P., Low,J.K., Webb,S.R., Silva,A.P., Mackay,J.P. and Shepherd,N.E. (2015) A peptide affinity reagent for isolating an intact and catalytically active multi-protein complex from mammalian cells. *Bioorg. Med. Chem.*, **23**, 960–965.
55. Reynolds,N., Salmon-Divon,M., Dvinge,H., Hynes-Allen,A., Balasooriya,G., Leaford,D., Behrens,A., Bertone,P. and Hendrich,B. (2012) NuRD-mediated deacetylation of H3K27 facilitates recruitment of polycomb repressive complex 2 to direct gene repression. *EMBO J.*, **31**, 593–605.
56. Rush,M., Appanah,R., Lee,S., Lam,L.L., Goyal,P. and Lorincz,M.C. (2009) Targeting of EZH2 to a defined genomic site is sufficient for recruitment of Dnmt3a but not de novo DNA methylation. *Epigenetics*, **4**, 404–414.
57. Margueron,R., Justin,N., Ohno,K., Sharpe,M.L., Son,J., Drury,W.J. 3rd, Voigt,P., Martin,S.R., Taylor,W.R., De Marco,V. *et al.* (2009) Role of the polycomb protein EED in the propagation of repressive histone marks. *Nature*, **461**, 762–767.
58. Cheng,A.W., Wang,H., Yang,H., Shi,L., Katz,Y., Theunissen,T.W., Rangarajan,S., Shivalila,C.S., Dadon,D.B. and Jaenisch,R. (2013) Multiplexed activation of endogenous genes by CRISPR-on, an RNA-guided transcriptional activator system. *Cell Res.*, **23**, 1163–1171.
59. Beerli,R.R., Segal,D.J., Dreier,B. and Barbas,C.F. III (1998) Toward controlling gene expression at will: specific regulation of the erbB-2/HER-2 promoter by using polydactyl zinc finger proteins constructed from modular building blocks. *Proc. Natl. Acad. Sci. U.S.A.*, **95**, 14628–14633.
60. Tang,X., Lowder,L.G., Zhang,T., Malzahn,A.A., Zheng,X., Voytas,D.F., Zhong,Z., Chen,Y., Ren,Q., Li,Q. *et al.* (2017) A CRISPR-Cpf1 system for efficient genome editing and transcriptional repression in plants. *Nat. Plants*, **3**, 17018.
61. Amabile,A., Migliara,A., Capasso,P., Biffi,M., Cittaro,D., Naldini,L. and Lombardo,A. (2016) Inheritable silencing of endogenous genes by hit-and-run targeted epigenetic editing. *Cell*, **167**, 219–232.
62. Bintu,L., Yong,J., Antebi,Y.E., McCue,K., Kazuki,Y., Uno,N., Oshimura,M. and Elowitz,M.B. (2016) Dynamics of epigenetic regulation at the single-cell level. *Science*, **351**, 720–724.
63. Tak,Y.G., Hung,Y., Yao,L., Grimmer,M.R., Do,A., Bhakta,M.S., O'Geen,H., Segal,D.J. and Farnham,P.J. (2016) Effects on the transcriptome upon deletion of a distal element cannot be predicted by the size of the H3K27Ac peak in human cells. *Nucleic Acids Res.*, **44**, 4123–4133.